

CEE 598 Advanced Computational Methods - Project 4

Javier A. Avecillas-Leon¹

¹Department of Civil and Environmental Engineering, University of Illinois at Urbana-Champaign, Urbana, IL 82060.

1 Strong form

Let us consider the two-dimensional incompressible Navier-Stokes equations

$$\begin{cases} \rho \left(\frac{\partial \mathbf{u}}{\partial t} + \mathbf{u} \cdot \nabla \mathbf{u} - \mathbf{b} \right) - \nabla \cdot \boldsymbol{\sigma} = \mathbf{0} \\ \nabla \cdot \mathbf{u} = 0 \end{cases} \quad (1)$$

where ρ is the fluid density and \mathbf{u} is the velocity vector field. The stress tensor $\boldsymbol{\sigma}$ is given by the following expression

$$\boldsymbol{\sigma} = -p\mathbf{I} + 2\mu\nabla^s\mathbf{u} \quad (2)$$

where p is the pressure field, μ is the fluid viscosity, and ∇^s stands for the symmetric gradient operator

$$(\nabla^s\mathbf{u})_{ij} = \frac{1}{2} \left(\frac{\partial u_i}{\partial x_j} + \frac{\partial u_j}{\partial x_i} \right) \quad (3)$$

2 Weak form

Considering a residual based variational multi-scale formulation, the weak form of the Navier-Stokes equation reads:

Find \mathbf{u}^h and p^h such that, for every \mathbf{w}^h and q^h , the following residual equation holds

$$\begin{aligned} R := & \left(\mathbf{w}^h, \frac{\partial \mathbf{u}^h}{\partial t} \right)_\Omega + (\mathbf{w}^h, \rho \mathbf{u}^h \cdot \nabla \mathbf{u}^h)_\Omega + (\mathbf{w}^h, \boldsymbol{\sigma})_\Omega - (\mathbf{w}^h, \rho \mathbf{b})_\Omega - (\mathbf{w}^h, \mathbf{h})_{\Gamma_h} \\ & + (q^h, \nabla \cdot \mathbf{u}^h)_\Omega + \sum_e [\nabla \mathbf{w}^h, \rho (\mathbf{u}^h \otimes \tau_M \mathbf{R}_M + \tau_M \mathbf{R}_M \otimes \mathbf{u}^h + \tau_M \mathbf{R}_M \otimes \tau_M \mathbf{R}_M)]_{\Omega_e} \\ & + \sum_e (\nabla \cdot \mathbf{w}^h, \tau_C \mathbf{R}_C)_{\Omega_e} + \sum_e (\nabla q^h, \tau_M \mathbf{R}_M)_{\Omega_e} = 0 \end{aligned} \quad (4)$$

Applying Crank-Nicolson to perform the time discretization, the time derivative of the velocity field is replaced by

$$\frac{\partial \mathbf{u}^h}{\partial t} := \frac{\mathbf{u}_{n+1}^h - \mathbf{u}_n^h}{\Delta t} \quad (5)$$

and all other quantities are evaluated at

$$\mathbf{u}_{n+1/2}^h := \frac{\mathbf{u}_{n+1}^h + \mathbf{u}_n^h}{2} \quad (6)$$

Due to the nonlinear nature of the problem, it is solved using a Newton-Raphson algorithm as follows¹

$$\mathbf{u}_{n+1} = \mathbf{u}_n - \Delta \mathbf{u}_{n+1}^k \quad (7)$$

where the ‘k-th’ increment of the solution vector ($\Delta \mathbf{u}_{n+1}^k$) is obtained by solving the following system

$$\mathbf{K}^T \Delta \mathbf{u}_{n+1}^k = \mathbf{R}_{n+1}^k \quad (8)$$

A *good approximation* of the consistent tangent matrix (\mathbf{K}^T) is obtained by neglecting the dependence of τ_R and τ_M on $\mathbf{u}^h(x, t)$ and taking the derivative of the residual vector with respect to the nodal coefficients. At the element level, this approach leads to

$$\mathbf{K}^T := \frac{\partial \mathbf{R}_{n+1}}{\partial \bar{\mathbf{u}}_{n+1}} \quad (9)$$

3 Finite element approximation

Let us establish an element approximation for the velocity field $\mathbf{u}^e(\mathbf{x}, t)$ and pressure field $p^e(\mathbf{x}, t)$ by means of polynomial shape functions

$$\begin{aligned} \mathbf{u}^e(\mathbf{x}, t) &\approx \mathbf{u}^h(\mathbf{x}, t) = \mathbf{N}_u^e(\mathbf{x}) \bar{\mathbf{u}}^e(t) \\ p^e(\mathbf{x}, t) &\approx p^h(\mathbf{x}, t) = \mathbf{N}_p^e(\mathbf{x}) \bar{\mathbf{p}}^e(t) \end{aligned} \quad (10)$$

where $\mathbf{N}_u^e(\mathbf{x})$ and $\mathbf{N}_p^e(\mathbf{x})$ denote the matrices of linear shape functions associated with element e used to interpolate the velocity and pressure field, respectively. Along the same lines, $\bar{\mathbf{u}}^e(t)$ and $\bar{\mathbf{p}}^e(t)$ denote the vector of element nodal velocity and pressure coefficients, respectively.

Similarly, the associated gradient quantities can be discretized using the corresponding \mathbf{B}_u^e and \mathbf{B}_p^e matrices, containing the derivative of the shape functions such that

$$\begin{aligned} \nabla \mathbf{u}^e(\mathbf{x}, t) &\approx \nabla \mathbf{u}^h(\mathbf{x}, t) = \mathbf{B}_u^e(\mathbf{x}) \bar{\mathbf{u}}^e(t) \\ \nabla p^e(\mathbf{x}, t) &\approx \nabla p^h(\mathbf{x}, t) = \mathbf{B}_p^e(\mathbf{x}) \bar{\mathbf{p}}^e(t) \end{aligned} \quad (11)$$

It is worth noting that considering the linearity of the shape functions, the term involving the Laplace operator in the weak form will be ignored. Finally, a similar discretization is adopted for $\mathbf{w}^h(\mathbf{x}, t)$ and $q^h(\mathbf{x}, t)$.

¹The superscript ‘h’ has been dropped to simplify the notation

4 Problem description

Let us consider the channel with plane walls illustrated in Figure 1 with dimensions $[0, 3] \times [0, 1]$. A fluid with properties $\rho_0 = 1.0$ and $\mu = 0.02$ passes over a wall with dimensions $[0, 2/75] \times [0, 0.4]$ located along the line $(x = 1, y)$. The problem adopts the following boundary conditions

- i) No interpenetration of the velocity field at the channel walls.
- ii) Inlet velocity field equal to

$$\begin{aligned} u_x(0, y, t) &= 0.5 \\ u_y(0, y, t) &= 0 \end{aligned} \tag{12}$$

The problem considers the following initial condition for the velocity field at the interior domain

$$\mathbf{u}(x, y, 0) = \mathbf{0} \quad \forall \mathbf{x} \notin \partial\Omega \tag{13}$$

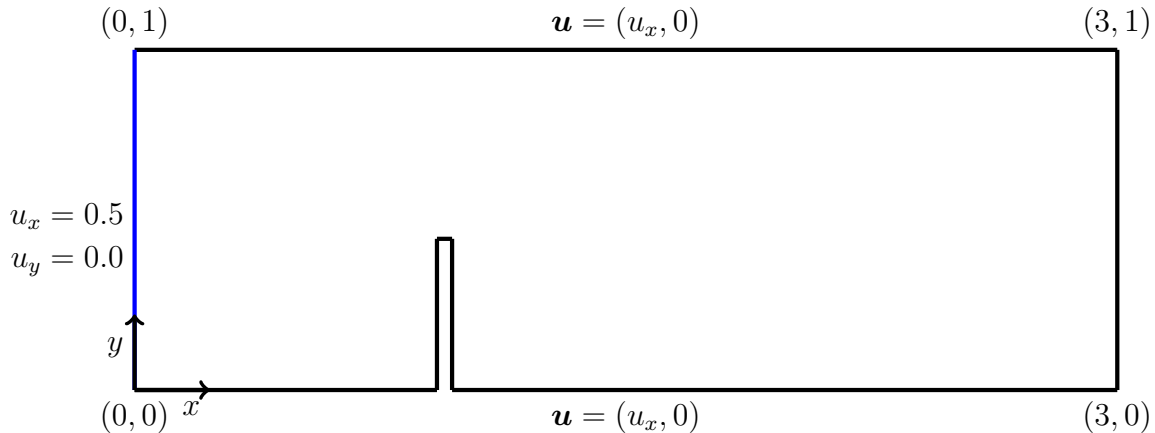


Figure 1: Domain representation and boundary conditions of the flow past a wall in a channel with plane walls

Finally, the simulation is run during $t_f = 5$ s with a time step equal to $\Delta t = 5e-03$ s. Figure 2 illustrates the finite element mesh used to discretize the problem domain. It is made of three-nodes linear triangular elements. Additional mesh refined was used around the wall to resolve in a more accurate way the velocity field.

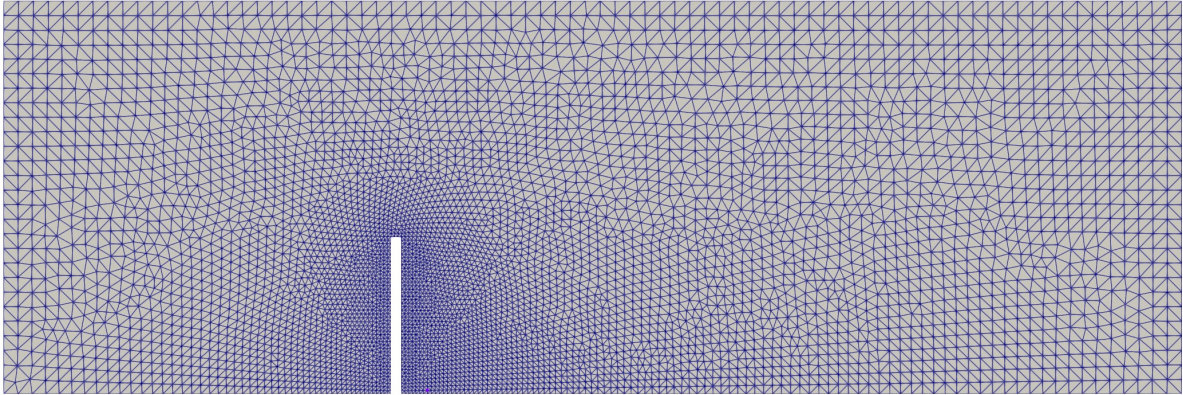


Figure 2: Finite element discretization of the problem domain using a mesh of three-node linear triangular elements

4.1 Numerical results

Figure 3 shows snapshots of the magnitude of the velocity and pressure fields at four instants of time. These results exhibit a velocity field with smooth behavior, which demonstrates that the numerical simulation is suitable to achieve stable solutions. Nevertheless, the accuracy of the numerically computed solution has not been tested. Additionally, the numerical simulation captures the unsteady flow that arises from a fluid moving past a obstruction, which is associated with the recirculating flow at the back of the wall. With regards to the pressure field, it is noted that it accumulates with time. This can be corroborated by looking at the maximum and minimum pressure values at each time step.

As mentioned previously, the accuracy of these numerical results has not been tested. During the solution of the nonlinear system of equations, there are load steps at which our implementation of the Newton-Raphson solver struggles to satisfy the convergence criterion $|\mathbf{R}_{n+1}^k| \leq 0.01|\mathbf{R}_{n+1}^0|$. This results in adopting the computed solution at the last iteration as the converged solution. The following are some potential improvements to the current setup that could lead to a better behavior of the nonlinear solver

- i) Provide inlet velocity boundary conditions that resemble a fully developed flow.
- ii) Provide a better estimate for the initial guess of the solution vector during the nonlinear solver.
- iii) Provide inlet or outlet boundary conditions for the pressure field.

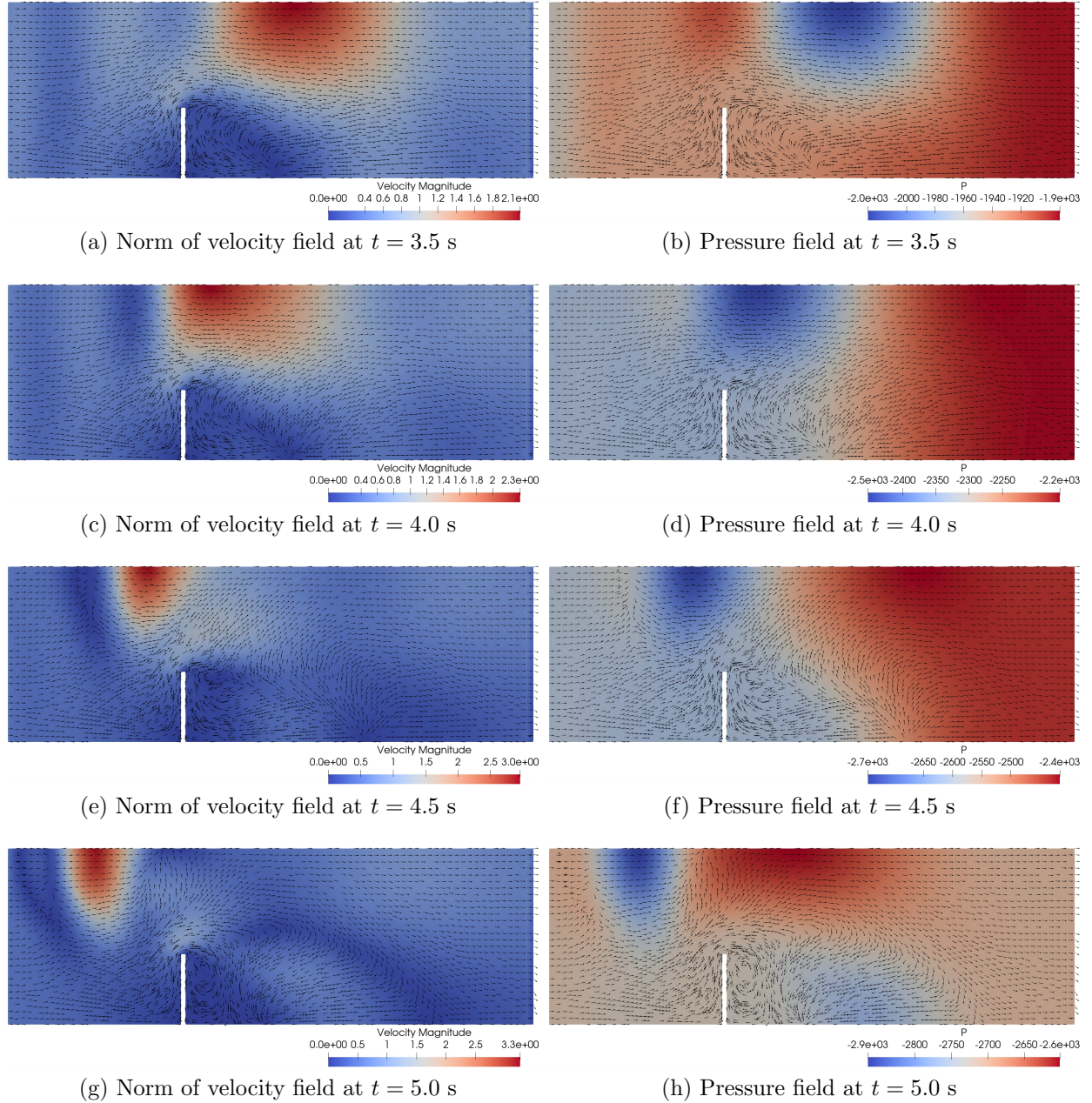


Figure 3: Norm of the velocity field and pressure field at different simulation times